Changes in Gut Viral and Bacterial Species Correlate with Altered 1,2-Diacylglyceride Levels and Structure in the Prefrontal Cortex in a Non-Human Primate Model of Depression.

Jing Wu
The First Affiliated Hospital of Chongqing Medical University
Tingjia Chai
Chongqing Medical University
Hanping Zhang
The First Affiliated Hospital of Chongqing Medical University
Yu Huang
The First Affiliated Hospital of Chongqing Medical University
Seth W Perry
State University of New York (SUNY) Upstate Medical University
Yifan Li
The First Affiliated Hospital of Chongqing Medical University
Jiajia Duan
The First Affiliated Hospital of Chongqing Medical University
Xunmin Tan
The First Affiliated Hospital of Chongqing Medical University
Xi Hu
The First Affiliated Hospital of Chongqing Medical University
Yiyun Liu
The First Affiliated Hospital of Chongqing Medical University
Juncai Pu
The First Affiliated Hospital of Chongqing Medical University
Haiyang Wang
The First Affiliated Hospital of Chongqing Medical University
Xin Jin
Stomatological Hospiral of Chongqing Medical University
Jinlin Song
Stomatological Hospital of Chongqing Medical University
Ping Ji
Stomatological Hospitao of Chongqing Medical University

Peng Zheng
The First Affiliated Hospital of Chongqing Medical University
Peng Xie (xiepeng@cqmu.edu.cn)
Chongqing Medical University https://orcid.org/0000-0002-5319-7842

Research

Keywords: major depressive disorder, Macaca fascicularis, gut microbiome, lipidomics, metagenomics

Posted Date: December 31st, 2020

DOI: https://doi.org/10.21203/rs.3.rs-136570/v1

Title

Changes in gut viral and bacterial species correlate with altered 1,2-diacylglyceride levels and structure in the prefrontal cortex in a non-human primate model of depression.

Authors

Jing Wu[1,2,3], Tingjia Chai[2,4]*, Hanping Zhang[1,2], Yu Huang[1,2], Seth W. Perry[5,6], Yifan Li[1,2], Jiajia Duan[2,3], Xunmin Tan[1,2], Xi Hu[1,2], Yiyun Liu[2], Juncai Pu[2], Haiyang Wang[2,7], Jinlin Song[7,8], Xin Jin[7,8], Ping Ji[7,8], Peng Zheng[1,2†] and Peng Xie[1,2†]*

Affiliations

[1]Department of Neurology, The First Affiliated Hospital of Chongqing Medical University, Chongqing, 400016, China

[2]NHC Key Laboratory of Diagnosis and Treatment on Brain Functional Diseases, The First Affiliated Hospital of Chongqing Medical University, Chongqing, 400016, China

[3]The M.O.E. Key Laboratory of Laboratory Medical Diagnostics, the College of Laboratory Medicine, Chongqing Medical University, Chongqing, 400016, China

[4]College of Biomedical Engineering, Chongqing Medical University, Chongqing, 400016, China

[5]Department of Psychiatry and Behavioral Sciences, College of Medicine, State University of New York (SUNY) Upstate Medical University, Syracuse, NY USA

[6]Department of Neuroscience & Physiology, College of Medicine, SUNY Upstate Medical University

[7]Chongqing Key Laboratory of Oral Diseases and Biomedical Sciences, Stomatological Hospital of Chongqing Medical University, 401147 Chongqing, China

[8]Key Laboratory of Psychoseomadsy, Stomatological Hospital of Chongqing Medical University

**These authors contributed equally to this study.*

[†]These authors are co-senior authors.

Corresponding authors

Professor Peng Xie; E-mail: xiepeng@cqmu.edu.cn

Professor Peng Zheng; E-mail: peng-zheng@foxmail.com

Abstract

Background: Major depressive disorder (MDD) is a debilitating mental disease, but its underlying molecular mechanisms remain obscure. Gut microbiome can modulate brain function and behaviors through the microbiota-gut–brain (MGB) axis in depression. Our previously established non-human primate model of naturally occurring depression-like behaviors, which is characterized by MGB axis disturbances, can be used to interrogate how a disturbed gut ecosystem may modulate the MDD onset. To better clarify the molecular interrelationships and downstream functional consequences in the MGB axis on MDD pathology, here, gut metagenomics were used to characterize how gut virus and bacterial species, and associated metabolites, change in depressive monkey model.

Results: We identified a panel of 33 gut virus and 14 bacterial species that could discriminate the depression-like (DL) from control *M. fascicularis*. In addition, using lipidomic analyses of central and peripheral samples obtained from these animals, we found that the DL macaque were characterized by alterations in the relative abundance, carbon-chain length, and unsaturation degree of 1,2-diacylglyceride (DG) in the prefrontal cortex (PFC), in a brain region-specific manner. In addition, lipid-reaction analysis identified more active and inactive lipid pathways in PFC than in amygdala or hippocampus, with DG being a key nodal player in these lipid pathways. Significantly, co-occurrence network analysis showed that altered gut viral and bacterial species, and their interaction may be relevant to the onset of negative emotions behaviors by modulating the DG levels in PFC in the depressive macaque.

Conclusions: Our findings suggest that altered gut virus and bacteria as well as DG levels and structure in the PFC are hallmarks of the DL macaque, thus providing a new framework for understanding the gut microbiome's role in depression.

Keywords: major depressive disorder, *Macaca fascicularis*, gut microbiome, lipidomics, metagenomics

Background

Major depressive disorder (MDD) is a serious mental disorder that imposes a substantial burden on families and society worldwide[1]. Currently, the underlying molecular basis of MDD remains uncertain. In addition, only a subset of patients with MDD are effectively treated by the currently available antidepressant drugs, which have been developed based on the existing theories for the molecular basis of MDD[2, 3] . Therefore, identification of new molecular mechanisms and more effective therapies for MDD are required.

Emerging evidence suggests that the gut microbiome can modulate brain function and behaviors through the microbiota-gut–brain axis (MGB), and plays a vital role in the pathogenesis of various mental disorders such as autism, bipolar disorder, and schizophrenia[4-7]. Recently, we and others found that patients with MDD had disturbed gut microbiomes, but the underlying mechanisms by which the gut microbiome may contribute to the pathogenesis of MDD are unclear. Previously, we established and reported a non-human primate(NHP) model of naturally occurring depression-like behaviors, which developed under conditions of chronic social dominance stress[8, 9]. This unique animal model replicates many characteristics of depression onset and behaviors in humans. This primate depression model was also characterized by MGB axis disturbances, thus providing an ideal model to investigate the gut ecosystem's roles in depression development.

Previously, integrated metabolomic and metagenomic analyses in these DL macaques found that their altered gut microbiota were associated with brain-region specific glycerophospholipid metabolism changes the prefrontal cortex

(PFC), amygdala (AMY), and hippocampus (HIP)[8]. Similar alterations were also found in the PFCs of germ-free mice that received fecal microbial transplants (FMTs) from MDD subjects[10]. Gut microbiota can influence MGB lipid and fatty acid production and metabolism, and lipid peroxidation and signaling pathway activation[11]. However, further studies are needed to better clarify the molecular interrelationships and downstream functional consequences of these changes on MDD pathology.

Lipids are a group of distinct biological molecules which make up over 50% of the brain's dry mass, and are vital participants in fundamental neurobiological processes including neuronal membrane synthesis, and vesicular and synaptic transmission and trafficking. There are major subclasses of lipids such as fatty acids; glycerolipids such as mono-, di-, and tri-acylglycerol (MG, DG, and TG, respectively); and glycerophospholipids such as phosphatidylcholine (PC), phosphatidic acid (PA), and phosphatidylglycerol (PG). In the brain, with various enzymatic reaction systems, lipids achieve rapid transformations across subclasses, and disrupted lipid transformations (and thus equilibrium) can manifest as a variety of neurological diseases[12, 13]. Moreover, the structures and dynamic activities of neural cells' membranes are profoundly sensitive to lipid structure, including acyl carbon chain length and unsaturation[14]. For neurons and glia, and their vesicles, changes in membrane permeability and fluidity, as regulated by lipid composition and structure, help control synaptic excitability and transmission, and the stabilization of ion channels[15, 16]. Short-chained and saturated lipids generate a more tightly packed and compressed cell membrane whilst, in contrast, longer-chained and unsaturated lipids occupy more space and are more mobile in membranes.

For these reasons, here we used shotgun metagenomic analysis of fecal samples, and mass spectrometry (MS) lipidomic analysis of brain regions (PFC,

AMY, and HIP) and plasma, from 12 female DL macaques (*Macaca. fascicularis*) and healthy controls (HC). With these well-established bioinformatic approaches, the differential gut virus, bacteria, and brain lipids between the DL and HC macaques were identified. Based on metabolic reactions among lipids, we identified the involved pathways and predicted the active or inactive lipid reaction pathways in key brain regions involved in MDD pathology. Finally, we integrated these multi-level omics findings by network analysis to connect and correlate the altered virus and bacteria with the observed DL behaviors, to further uncover how these disturbed signatures may modulate the host's metabolism and behavioral function.

Methods

Ethics Statements

Detailed ethics approvals were shown in Declaration. In brief, this study was performed in strict accordance with the recommendations in the "Guide for the Care and Use of Laboratory Animals" of the Institute of Neuroscience at Chongqing Medical University (#20100031). The sample sizes (n=6/every group) were chosen based on the data of previous NHP studies [17, 18], and our previous works on behavior and biochemical measures in *M. fascicularis*[19]. Macaques were housed in an environmentally controlled facility (22 ± 1 ^{o}C temperature; 50 ± 5% relative humidity; and 12h light/12h dark cycle with lights on at 7:00 AM).

Behavioral observation and tissue preparation

We identified *M. fascicularis* animals with naturally occurring DL behaviors as described previously[8, 19]. Briefly, we surveyed the populations from 20 enclosures, and identified 6 typical DL and 6 HC macaques. All 12 identified macaques were adult female and disease-negative by veterinary examination.

The DL behaviors Huddle, Sit alone, Locomotion, and Amicable were observed and identified via “free enclosures tests”[20]; the behavior Communication was evaluated and identified by “social interaction test”. The “free enclosures test” was conducted within the macaque’s native habitat housing, via video records collected for 20-30 min per shoot, with 6-7 replicates over 3 days. The “social interaction test” was performed in isolated cages, with video records collected for 30 min per shoot with 2 repeats. Based on the similarity with human emotions, behaviors Huddle and Sit alone were identified as negative emotions, behaviors Locomotion, Amicable and Communication were identified as positive emotions. All behavioral observations were videotaped and analyzed by NOLDUS Observer XT software (version 10.0, Noldus Information Tech Technology, Leesburg, PA). The detailed behavioral results have been published previously[8, 19, 20]. Following euthanization, whole brains were isolated and immediately frozen in liquid nitrogen, and cut into 5mm slices along the coronal plane[21, 22]. The PFC, HIP, and AMY were dissected according to a macaque brain atlas [23, 24], then stored at -80 ^{o}C until use.

Metagenomic analysis of fecal samples

The metagenomic libraries were prepared and sequenced according to our previous protocols[25, 26]. Briefly, we extracted microbial DNA from the 6 DL and 6 HC macaque fecal collections using the E.Z.N.A. Stool DNA Kit (Omega Bio-tek, Norcross, GA, USA). The DNA extract was sheared using Covaris M220, aimed insert size was about 300 bp. A paired-end library was constructed using TruSeqTM DNA Sample Prep Kit (Illumina). Then, the amplicons library was paired-end sequenced on an Illumina HiSeq X platform[27]. Threshold exclusion in sequence quality control and genome assembly was performed as we described previously[25, 26]. Reads were aligned to the macaque (*Macaca fascicularis*) genome by BWA (http://bio-bwa.sourceforge.net), and any hit

associated with the reads and their mated reads were removed. Metagenomics data were assembled using MEGAHIT [28](https://github.com/voutcn/megahit), contigs with the length being or over 300 bp were selected as the final assembling result. All predicted genes with a 95 % sequence identity (90% coverage) were clustered using CD-HIT[29] (http://www.bioinformatics.org/cd-hit/). Reads after quality control were mapped to the representative sequences with 95% identity using SOAPaligner[30] (http://soap.genomics.org.cn/). Here, prior to construction of gene sets, we initially removed the host sequences with high homology to the macaca genome from microbial metagenomes. Based on the NCBI NR database, we annotated gene sets for bacteria, fungi, viruses, protozoa, and archaea using Diamond (Version 0.8.35). Based on a unified database, each gene is assigned to the highest scoring taxonomy, which facilitates simultaneous assessment of these microbial species in the gut ecosystem of depressive macaca [31]. The differential bacterial species and gut viruses between the two groups were identified using Linear discriminant analysis (LDA) Effect Size (LEfSe) with an LDA score >2.0[32].

Lipid identification and analysis

Details of the lipidomic methods were based on LC-MS/MS, similar to our previously published protocols[8, 26]. Briefly, brain tissue samples were prepared by homogenization, dissociation, and centrifugation, and plasma samples were collected and centrifuged twice[25]. Chromatographic conditions: the column is Hypersil GOLD C18 (100×2.1mm, 1.9μm); the mobile phase A is acetonitrile: water (60:40, V/V), mobile Phase B is acetonitrile: isopropanol (10:90, V/V); the flow rate was 0.40 mL/min, the injection volume was 5 μl, and the column temperature was 45°C. Mass spectrometry was conducted using Thermo Scientific™ Q Exactive™ quadrupole-qrbitrap mass spectrometer.

Mass spectrometry peaks were identified using the Thermo Scientific™

LipidSearch™, which contains over 150 million lipid species. Sample names, lipid information (species, subclass, structural information), and normalized peak area percentages, were integrated and imported into SIMCA-P+14.0 (Umetrics, Umeå, Sweden). Discrimination of lipid species between DL and HC samples was analyzed and visualized using partial least squares discriminant analysis (PLS-DA)[33]. To identify the differential lipid species responsible for discriminating between the two groups, we used threshold of variable importance plots (VIP) > 1.0 with statistical significance set at $P < 0.05$.

Lipid reaction activities in lipid pathways

The reaction activities in lipid pathways can be predicted based on methods as described previously[34, 35]. This method calculated statistical *Z* scores for all possible lipid pathways in order to predict whether a particular pathway is active or inactive in DL as compared to HC. Reactions with higher *Z* scores were identified as active. First, we examined all possible lipid pathways from Reactome (http://www.reactome.org/) and constructed a pathway network. Based on the pathway network, we computed the reaction weight vector ()as a ratio of product (A_{i+1}) over substrate (A_i) for each edge in the network ($\omega_i = (A_{i+1}/A_i)(i = 1,2,\dots,k-1)$). Then, for each weighted edge of the pathway, one-sided Student's t-tests were performed using the weights between DL and HC, to identify reactions with differential activity. By assuming that the t-distribution can be approximated by a normal distribution, the *P* values were converted to *Z* scores using the cumulative distribution function *CDF*, $Z=CDF^{-1}(1-P)$. We chose the significance level (*P*) to be 0.05, corresponding to a Z_i > 1.645 for a reaction to be considered as significantly active. For visualization, the *Z* scores were multiplied by -1 for the reactions which were significantly more active in HC as opposed to DL. Finally, we calculated an average *Z* score for lipid pathways to detect consistent changes in the flux across multiple reaction steps.

Z score for pathway A (Z_A) was calculated by all $Z_i (i = 1,2, \dots, k-1)$ of reactions in the pathway, as follows:

$$Z_A = \frac{1}{\sqrt{k-1}} \sum_{i=1}^{k-1} Z_i$$

As shown in references [34, 35], Z_A also follows a normal distribution. To determine if pathway A was significantly more active, we again chose the significance level (*P*) to be 0.05, corresponding to a Z_i > 1.645 for reaction to be considered as significantly active. Again, these *Z* scores were multiplied with -1 for the reactions which were significantly more active in HC as opposed to DL. For visualization, a negative *Z*-score indicates inactive pathway in DL relative to HC, and a positive *Z*-score indicates active pathway in DL relative to HC.

Statistical analyses

Statistical analyses were carried out using SPSS (version 21) and R studio (version 3.5.2, 2018), unless otherwise described. The discriminating lipid species between the two groups were considered significant at the threshold of VIP > 1.0 and P-values < 0.05. The levels of all lipid subclasses were analyzed by unpaired two-tailed Student's t-tests. Error bars represent the standard error of the mean (SEM) in all cases. LEfSe analysis was used to identify the different gut bacteria and viruses by estimating the effect of the abundance of each species (LDA > 2 and P value < 0.05). In established lipid pathways, the reactions were considered as significantly active (or inactive) for their calculated Z score > 1.645 (or < -1.645), corresponding to the P-value < 0.05. Correlation data analysis was performed using the spearman's regression model with the significance threshold of P < 0.05. The investigators were not blinded to the group classification while analyzing the data.

Results

Gut virus differences between DL and HC macaques

The obtained metagenomic sequencing was mapped to the known viral genomes NCBI NR database. From the filtered sequence data, we annotated 1311 viral species based on the NR database. Using LEfSe analysis, we identified 33 differential gut viral species that could discriminate between the DL and HC groups (**Figure 1a, Supplemental Table 1**). Compared to HCs, the DLs were characterized by 16 enriched gut viruses, mainly belonging to the *Myoviridae* (7 species) and *Siphoviridae* (4 species) families, and 17 depleted viruses mainly from the *Podoviridae* (6 species) and *Siphoviridae* (6 species) families. Interestingly, the majority of altered gut viruses (25/33, 75.76%) belonged to the order *Caudovirales*, suggesting altered *Caudovirales* ecology was a hallmark of the DL animals.

Gut bacterial species differences between DL and HC macaques

Here, using our previously published metagenomic data[8], we reannotated 468 bacteria families and 11653 species based on NR database. Using LEfSe analysis, we identified 14 differential gut bacterial species responsible for distinguishing the DL and HC groups (**Figure 1b**, **Supplemental Table 2**). Compared to the HC group, the DL group was characterized by 6 increased bacteria species, mainly belonging to the *Paraprevotella* family (3 species), and 8 decreased species mainly from the *Streptococcaceae* (3 species) and *Gemella* (3 species) families. The majority of altered bacterial species (9/14, 64.28%) belonged to the phylum Firmicutes.

DL macaques have different lipid composition in plasma and depression relevant brain regions

In total, we identified 2238, 2153, and 2074 lipid species in PFC, AMY, and HIP, respectively. The proportions of lipid subtypes between brain regions were

generally similar, with phosphatidylethanolamine (PE), PC, and phosphatidylserines (PS) being the most abundant species in each region, together comprising 67.7%, 68.7%, and 68.2% of all lipid species in PFC, AMY, and HIP respectively (**Figure 2a**). Lipid species found in plasma were mainly comprised of PE, PC, and triacylglycerol (TG) subtypes, together comprising 65.8% of the 1591 lipid species found in plasma (**Figure 2a**). PLS-DA was performed to determine whether the overall lipidomic signatures of DL macaques were significantly different from those of controls. These lipidomics assays identified robust differences between HCs and DLs in PFC, AMY, HIP, and plasma (**Figure 2b**).

DL macaques have different lipid levels and structure in plasma and depression relevant brain regions

We compared the relative abundance of each lipid subclass between DL and HC, and found that there were specifically altered lipid subclasses in the same three brain regions. Normalizing against the corresponding lipid level in HCs, we found DG was significantly increased in PFC (FC=1.38 , P=0.0008) (**Figure 3a**), PA was significantly increased in AMY (FC=1.18, P=0.04) (**Figure 3b**), and monosialotetrahexosylganglioside (GM1) was significantly increased in HIP (FC=1.51 , P=0.04) (**Figure 3c**). Then we further identified the discriminating lipid species between DL and HC macaques using double cut-off (results were considered statistically significant if $P < 0.05$ and VIP > 1.0). Of the 72 total discriminating lipid species, we found that HIP had the most (28 species), while AMY had the least (7 species) (**Supplemental Figure 1**). These results were consistent with what we previously reported based on untargeted metabonomics[8].

DG lipid structure is altered in depression relevant brain regions of DL macaques

Brain function relies on the homeostasis of cellular membranes, and its perturbation might partially explain the neuronal deficits found in depression. The carbon chain length and the degree of unsaturation of fatty-acyls are two key elements of lipid architecture that impact membranes' functional biophysical properties. Our lipidomic analyses demonstrated not only differences in relative lipid composition and levels between HC and DL macaques, but also differences in lipids' biochemical structures with potential structure-function consequences on neural cell activity. Among the altered lipid subclasses, DG showed profound structural alterations, with multi-level alterations of carbon chain length and degree of unsaturation. Compared with HC, the DL macaques had altered levels of DGs with carbon chain lengths of 34C, 36C, and 43C in PFC, and 38C in AMY and HIP (**Figure 3d**). The differential carbon chain length DGs were primarily in the range of 34C to 40C, a range which comprised the majority of DG species. We also analyzed the degree of unsaturation for each subclass and DG. Compared with HCs, the degree of unsaturation of DG was significantly increased in 2, 3, and 10 double bones in PFC, but there was no difference in unsaturation degree of DG in AMY or HIP (**Figure 3e**). Taken together, DG structure and degree of unsaturation was the most different in the PFC, in HC versus DL macaques.

In the periphery (plasma), the structural changes in DG species were distinctly different than seen in brain. In plasma, the typical DG carbon chain length was longer, mainly 62C to 67C (**Figure 3d**). The degree of unsaturation was lower, mainly 0 to 3 (**Figure 3e**), compared with 2 to 6 carbon bones of DG in brain. There were no difference in carbon chain length or unsaturation degree in plasma DG.

DG-related lipid pathway activity was altered in DL macaques

Given the altered abundance and structure of brain DG, next we employed lipid-reaction analyses to explore whether specific lipid pathways were dysregulated in key depression-relevant brain regions in the DL macaque. Based on the Reactome and KEGG databases, we measured each lipid reaction and mapped them into lipid pathways. Briefly, the upstream and downstream transformations of any lipid species can be viewed as an edge, that can be evaluated by statistical *Z*-scores for predicting active and inactive pathways. Using a significance level of $P = 0.05$, corresponding to $Z > 1.645$ for a reaction to be considered significantly activated, we found altered lipid pathway activity in PFC, HIP, and AMY. In the PFC of DL macaques, 3 lipid pathways were significantly activated (LPC-PC-PA-DG-TG, LPC-PC-PA-LPA, and LPC-LPA), and 2 lipid pathways significantly inactivated (DG-PC-LPC, DG-PA-PI-LPI) relative to HCs (**Figure 4a-c**). In the HIP, the LPC-LPA pathway was activated, and the LPA-PA-PG-LPG pathway inactivated, in DL versus HC. (**Figure 4b, c, Addition file 2 Figure S2a**). LPC-LPA activity was significantly increased in both PFC and HIP (**Figure 4b**), but otherwise no lipid pathway activity was significantly changed across more than one brain region examined (**Figure 4b, 4c**). This most dysregulation of lipid pathway activity occurred in PFC (3 active, 2 inactive, in DL relative to HC), followed by HIP (one up, one down) (**Figure 4b, 4c**).

We also calculated *Z*-scores for synthesis and degradation of DG and PA. Interestingly, for DL relative to HC, we found significantly activated synthesis and inactivated degradation of PA in the AMY (**Addition file 2 Figure S2c, S2d**, respectively), which corroborates the higher PA levels in DL AMY as measured by MS (**Figure 3b**). However, the accumulation of DG in the DL PFC (**Figure 3a**) appears to arise principally from inactivated degradation, although DG synthesis in the DL PFC trended toward an increase but was not significant

(**Addition file 2 Figure S2c, S2d**, respectively).

Next, we explored the molecular geometry of lipids in these altered pathways and found some interesting lipid shape changes in these altered lipid pathways in the PFC of the DL macaques. Based on the size ratio of the hydrophilic head to the hydrophobic tail**,** glycerophospholipids and glycerolipids can be classified into cone (small head, two or more hydrophobic tails; including DG, PA, and TG), cylinder (large head and two hydrophobic tails; including PC and PI), or inverted cone (large head and single hydrophobic tail; including LPI and LPC) shapes. As shown in **Figure 4f**, the altered lipid pathways tend to promote (red arrow) lipid shape evolution from inverted cone lipids to cylinder and cone lipids, and to inhibit (blue arrows) the opposite evolution. DG lay at the intersection of these evolutions of lipid molecular geometry, and was involved in multiple processes.

Co-occurrence network analysis of changes in gut viruses, bacteria, and DG levels in DL macaques versus HCs.

To explore the potential interactions of these microbiome and molecular changes along the MGB axis of DL macaques, we constructed co-occurrence networks of altered gut viruses, bacteria, and DG in the PFC of DL versus HC macaques. Using an edge-weighted spring-embedded layout, the network was visualized and the nodes were spontaneously mutually attractive or exclusive based on the coefficient between nodes (**Figure 5**). Overall, co-occurrence analysis showed that gut viruses and bacteria formed strong and broad co-occurring relationships with DG levels in PFC; and the five behavioral phenotypes were divided, and the other nodes were spontaneously clustered with positive covariation around the behaviors. In the left region of this generated co-occurrence network, we found that two viral clusters (*Myoviridae* (#1), *Siphoviridae* (#3)) and a bacterial cluster (*Prevotellaceae* (#2)) were

directly or indirectly substantially correlated with 11 DG species in PFC; meanwhile, those altered DG species in PFC of DL macaque were positively correlated with negative emotions behaviors (Huddle and Sit alone). In the right region of this network, alternations of two viral clusters (*Siphoviridae* (#6), *Podoviridae* (#4)) and two bacterial cluster (*Gemella* (#5), *Streptococcaceae* (#7)) were substantially correlated with Communication and Locomotion behaviors. Meanwhile, only one DG species in PFC was positively correlated with the two positive emotions behaviors. In addition, there were no gut viral or bacterial clusters distributed around the Amicable behavior node. Together, our findings suggest that altered gut viral and bacterial species, and their interaction may be relevant to the onset of negative emotions behaviors by modulating the DG levels in PFC in the non-human primate model of depression.

Discussion

Growing evidence suggests that disturbed gut microbiome may contribute to depression pathology, but the specific mechanisms remain unclear. Here, we combined metagenomic and brain lipidomic analyses of *M. fascicularis* macaques with naturally occurring depressive behaviors. We identified 33 altered viral species mainly belonging to *Myoviridae*, *Podoviridae,* and *Siphoviridae*, and found 14 altered bacterial species mainly belonging to *Paraprevotella*, *Streptococcaceae*, and *Gemella*. In the brain, we found marked disturbances of DG levels and structure in the PFC of DL macaques compared to controls. Moreover, lipid reaction networks identified more activated and inactivated lipid pathways in PFC than in AMY or HIP, with DG being a key nodal player in these PFC lipid pathways. Finally, co-occurrence analysis showed that altered gut viral and bacterial species, and their interaction were correlated with onset of negative emotions behaviors by modulating the DG levels in PFC.

Previously, the role of the gut virome has been unexplored in depression.

However, importantly, we found that our DL animals had more altered gut viruses than gut bacteria, suggesting that the gut virome may play a role at least equivalent to that of the gut bacteriome in the pathology of depression. The three differential viral families were bacteriophages associated with gut bacteria, suggesting that such viruses may influence host behaviors via regulating their host bacteria. In the DL macaques, the altered phages mainly parasitize *Proteobacteria* and *Firmicutes* bacteria. Interestingly, we recently found similar viral disturbances in MDD patients[36], in which the altered gut viruses were mainly bacteriophages too. The MDD patients had increased *Siphoviridae* but decreased *Podoviridae* viral family populations, which aligns with our findings in the DL macaques described herein. These findings firmly establish the importance of further research on gut viruses' potential role in depression, and emphasize that such phage disturbances may be both a hallmark and diagnostic of depression.

Recent clinical investigations have reported significant changes of gut microbiome in patients with MDD. These clinical findings were partly inconsistent due to the demographic diversity of cohorts and analytical approaches. Our NHP depressive model used herein provided an ideal model to avoid those confounding factors, due to the native social structure and habitat that are characteristic of this model. Like many other reports of the depression microbiome[25], we again identified disturbances of the phylum *Firmicutes*. The enriched microbiota in the DL macaques mainly belonged to the family *Paraprevotella*, and the depleted species mainly belonging to the genera *Gemella* and *Streptococcus*. *Paraprevotella* has been suggested as a biomarker in depression[37, 38] and attention deficit hyperactivity disorder[39], as well as a potential factor to inhibit plasma acetate levels and intrarenal RAS activation[40]. *Streptococcus* strains such as *Streptococcus salivarius* and *Streptococcus thermophilus*, previously recognized as pathogens, have

recently been used as psychobiotics in mental health [41-43]. In our study, we also found some *Streptococcus* enriched in healthy controls, suggesting that gut *Streptococci* may play protective roles in the MGB axis.

Brain is particularly enriched in lipids, with a diverse lipid composition compared to other tissues[44]. Changes in the composition and structure of lipids in the brain profoundly affect neurodevelopment and signal transduction in perception and emotional behavior, which may lead to depression and anxiety disorders[45-47]. Previous lipidomic studies mainly focused on the amount of the different lipid species, which is reasonable but there are still some limitations: the variation of lipid structure and abundance. Recent studies have tried to scrutinize the structural and biotransformational alteration of lipids in disease. In our study, using a comprehensive approach, we tried to identify a key lipid group along the MGB axis that may be relevant to depression. DG in PFC was identified based on 4 aspects: first, the abundance of DG was significantly higher in PFC; second, the carbon chain length and unsaturation of DG were altered in at multiple levels; third, DG pathway activity was profoundly altered in PFC; last, DG in PFC was deeply involved in the MGB axis-behavior network.

In our previous studies and other preclinical and clinical experiments, disturbances of glycerolipid and glycerophospholipid metabolism were considered hallmarks in depression[48-51], but their role in depression pathogenesis is not explicitly clear. Here, using lipidomic approaches, we further showed alterations in DG pathway lipid shapes especially in the PFC of DL macaques. Both DG-related reaction pathways showed shape transformations from inverted cone and cylinder to cone via decreased headgroup size and more hydrophobic tails. Previous studies have reported that changes in bilayer curvature during vesicle fusion/fission relies on lipid shapes via CHOL translocations (chains)[14, 52, 53]. The cone shaped lipids,

462 mainly PA and DG, promote negative membrane curvature via various
463 phospholipases, while lyso-phosphatidylcholine (LPC) has only a single
464 hydrocarbon tail that promotes positive membrane curvature[53]. Secondly,
465 emerging evidences shows that the fatty acid chain length and unsaturation are
466 involved in anxiety and cognitive disorders by modulating membrane fluidity[54,
467 55]. Here we found that the unsaturation degree of DG in PFC was altered, and
468 the di- and tri-unsaturated DG significantly decreased, suggesting that the low
469 unsaturated fatty acids may weaken the protection of poly-unsaturated fatty
470 acids (PUFAs) in depression. As Levental et al. recently reported[56],
471 exogenous PUFAs such as docosahexaenoic acid (DHA) and ω-6 arachidonic
472 acid (AA) can reduce the di- and tri-unsaturated lipid species by counteracting
473 cell membrane perturbations. Together, these findings may extend our
474 understanding of brain lipids on depression.

475 It is widely accepted that gut microbiota can modulate hosts behaviors via
476 the MGB-axis. Here we also confirmed that robust network correlations occur
477 amongst the integrated gut virus, gut bacteria, and DG changes in the PFC of
478 DL macaques, and host DL behavioral phenotypes. Interestingly, virus and
479 bacteria were spontaneously clustered, and those clusters as well as DGs
480 surrounded different kinds of behaviors, suggesting the potential modulation
481 between viruses, bacteria, and depressive behaviors. Other studies have
482 shown phages interfere with host bacteria. For example, Loeffler et al. found
483 that *Podoviridae phage C1* can kill A, C, and E *streptococci* via lytic
484 enzymes[57]. Romero et al. further confirmed that *Siphoviridae phiHER* can kill
485 *Streptococcus pneumoniae* by specifically cleaving covalent bonds of cell wall
486 peptidoglycan[58]. In line with these findings, in our results the *Podoviridae* (#4)
487 and *Siphoviridae* (#6) virus clusters co-localized with the bacterial cluster
488 *Streptococcaceae* (#7). These studies confirm that gut microbiota can modulate
489 the host lipid metabolism in various ways, which may offer new therapeutic

avenues for depression.

Interestingly, the five behavioral phenotypes of our DL macaque were spontaneously separated: Huddle and Sit alone, which can represent negative emotions and unhealthy affect in macaque, co-localized with the majority of DG species, and with 3 microbial clusters; Locomotion and Communication, which can represent positive emotions and healthy affect in macaque, were co-localized with only 1 species of DG and 4 microbial clusters; but Amicable, another positive emotional behavior, located alone. These findings confirmed the reliability of our previously established behavior spectrum, and strongly suggested that the gut microbiota and brain lipids may modulate positive or negative emotion in different ways in depression. In our findings, DG mainly correlated with negative emotions rather than with positive emotions, suggesting that functional behavioral disturbances caused by changes in DG species composition, levels, and/or structure may serve to regulate or exacerbate negative emotions in depression. In contrast, positive emotions in depression may be modulated by the other unknown lipid groups. Interestingly, the unique DG species (DG (22:6/22:6)) that co-localized around positive emotions in our network analysis, is made up with a well-known fatty acid-docosahexaenoic acid (DHA). Many studies have investigated DHA supplementation as a potential treatment or prophylatic for depression. Van der Burg et al. found that DHA concentrations in red blood cell membranes were significantly correlated with a decrease in depressive symptoms during active treatment, and increased in response to depression treatment[59]. Weiser et al. fed pregnant rats with diets sufficient or deficient in DHA during gestation and lactation, and found that depressive-like behavior and its associated biomarkers in DHA-deficient offspring were worse compared with animals with sufficient levels of DHA[60]. In both these studies, the fatty acids were ingested, meaning that gut microbes would have participated in the absorption of these

518 dietary fatty acid supplements. Based on our and these results, further studies
519 of the intertwined roles of the gut microbiome and lipids in the pathology and
520 pathogenesis of depression are warranted.

521 Nonetheless, there are some limitations of our study, which can also
522 provide direction for future research. First, due to the low reproductive rate and
523 morbidity, as well as ethical considerations, the sample sizes were relatively
524 small, thus the reliability of the association reported may be impacted. Second,
525 the effects on key viruses, bacteria, and brain lipids that we reported in this
526 study need further longitudinal independent validations with larger samples.
527 The key viruses and bacteria need further isolation and culturing from macaque
528 fecal samples, and more independent verifications in multiple animal models,
529 such as fecal microbiota transplantation (FMT) or microbial agents. Third,
530 depression as a complex mental disorder, and depression pathology is not
531 isolated to only the PFC, HIP, and AMY regions studied here (although those
532 are key regions of depression neuropathology). Thus further studies with
533 broader brain regions and technologies such as FMRI, calcium imaging, and
534 optogenetics are needed. Fourth, MGB crosstalk in depression involves
535 multiple mechanisms and metabolic pathways beyond those which we focused
536 on in this study. The vagus nerve, hypothalamic–pituitary–adrenal axis, and
537 neuroimmune mechanisms, are all worthy of further study.

538 **Conclusions**

539 Taken together, using metagenomic data, we found the altered gut virome,
540 especially bacteriophages, plays a role in the onset of depression. Through
541 multiomics approaches, we have presented evidence that DL macaques were
542 characterized by disturbances of gut-virus, bacteria, and DGs in the PFC.
543 Moreover, we found that disturbances of gut microbiome may be relevant to the
544 onset of negative emotions behaviors by modulating the DG levels in the

depressive model. Our findings provide new directions to uncover the pathogenesis of depression.

Abbreviations

MDD: Major depressive disorder; DL: Depression-like; HC: healthy controls; PFC: Prefrontal cortex; NHP: Non-human primate; MGB axis: Microbial gut - brain axis; AMY: Amygdala; HIP: Hippocampus; FMTs: Fecal microbial transplants; MS: Mass spectrometry; LDA: Linear discriminant analysis; LEfSe: Linear discriminant analysis Effect Size; VIP: Variable importance plots; SEM: Standard error of the mean; PC: Phosphatidylcholine; PE: Phosphatidylethanolamine; Cer: Ceramide; LPE: Lyso-Phosphatidylethanolamine; PA: Phosphatidic acids; PG: Phosphatidylglycerols; PI: Phosphatidylinositols; PS: Phosphatidylserines; SM: Sphingmyelin; DG: 1,2-Diacylglycerol; LPC: 2-Lysophosphatidylcholine; So: Sphingosine; TG: Triacylglycerol; DHA: Docosahexaenoic acid; AA: ω-6 arachidonic acid

Declarations

Ethics approval and consent to participate

This study was performed in strict accordance with the recommendations in the “Guide for the Care and Use of Laboratory Animals” of the Institute of Neuroscience at Chongqing Medical University (#20100031). All work involving NHPs was conducted in accordance with the NIH guide for the care and use of laboratory animals (https://www.ncbi.nlm.nih.gov/books/NBK54050/) and with the recommendations of the Weatherall report, “The use of non-human primates in research”[61]. We also followed nc3r recommendations (https://www.nc3rs.org.uk/) by using the minimum number of depressed macaques and age-matched controls, while maintaining statistical reliability. The sample sizes (n=6/every group) were chosen based on the data of previous NHP studies [17, 18], and our previous works on behavior and biochemical measures in *M. fascicularis*[19]. The *M. fascicularis* facilities, housing, and primate laboratories used in this study are accredited by the Association for Assessment and Accreditation of Laboratory Animal Care. Macaques were housed in an environmentally controlled facility (22 ± 1℃ temperature; 50 ± 5% relative humidity; and 12h light/12h dark cycle with lights on at 7:00 AM). This study does not involve the use of human subjects.

Acknowledgements

Not applicable.

Funding

This work was supported by the National Key R&D Program of China (2017YFA0505700 and

2016YFC1307200), Non-profit Central Research Institute Fund of Chinese Academy of Medical Sciences (2019PT320002), Projects of International Cooperation and Exchanges NSFC (81820108015), the Natural Science Foundation Project of China (81971296, 81771490, 81371310, and 81200899), and Chongqing Science & Technology Commission (cstc 2019 jcyjjqX0009).

Author Contributions

Designed the experiments: P.X. and P.Z. Performed the metagenomic analysis: J.W., T.J.C., H.P.Z., J.L.S., X.J., P.J. and Y.F.L. Performed the lipidomic analysis: J.W., T.J.C., Y.H., and J.J.D. Analyzed the lipidomic and metagenomic data: J.W., X.M.T., J.C.P and X.H. Animal behaviors: J.W., Y.Y.L, and Y.H. Drafted the manuscript: P.X, and P.Z. Revised the manuscript for intellectual content: P.X., S.W.P., and P.Z..

Competing interests

The authors have declared no conflict of interest in the submission of this manuscript.

Availability of data and materials

The metagenomics data of macaque that support the findings of this study are available from The First Affiliate Hospital of Chongqing Medical University and have published previously [8]. All the lipidomics data analysed during this study are included in this published article and supplementary information files.

Consent for publication

Not applicable.

Competing interests

Not applicable.

FIGURES

Fig.1 The virus and bacteria that discriminate DL from HC groups

LEfSe of bacteria and virus from phylum to species level. Linear discriminant analysis (LDA) combined with effect size measurements revealed a list of features that enable discrimination between the HC and DL groups in the fecal samples. **a.** At the viral level, the DL subjects showed 16 enriched species, mainly belonging to families *Myoviridae* (7 species) and *Siphoviridae* (4 species), and 17 depleted species mainly from the families *Podoviridae* (6 species) and *Siphoviridae* (6 species). b. At the bacterial level, the DL subjects showed 6 enriched species, mainly belonging to family *Paraprevotella* (3 species), and 8 depleted species mainly from the families *Streptococcaceae* (3 species) and *Gemella* (3 species). The discriminative variants (gut virus, bacteria species) were identified based on LDA score > 2.5. Sample set: HC, n = 6; DL, n = 6.

Fig.2 Profile of lipidomic changes in brain and plasma.

a. Composition of subclasses of total identified lipids in prefrontal cortex (PFC), amygdala (AMY), hippocampus (HIP) and plasma. Identified lipids exhibited similar composition of subclasses in 3 brain regions (2238, 2153, 2074, respectively). **b.** Partial Least Squares Discriminant Analysis (PLS-DA) showed that the PFC, HIP, AMY and plasma metabolic signatures of DL group were substantially different from that in the HC group (n=6, HC, blue dots; n=6, DL, red dots). PC, Phosphatidylcholine; PE, Phosphatidylethanolamine; Cer, ceramide; LPE, lyso-Phosphatidylethanolamine; PA, phosphatidic acids; PG, phosphatidylglycerols; PI, phosphatidylinositols; PS, phosphatidylserines; SM, sphingmyelin; DG, 1,2-Diacylglycerol; LPC, 2-Lysophosphatidylcholine; So, sphingosine; TG, Triacylglycerol.

Fig.3 Significant changes exhibited in abundance and fatty acid composition of 1,2-Diacylglycerol (DG) in the PFC of DL macaques.

(a-c) The abundance of some lipidomic subclasses showed significantly changes with specific brain regions, displaying the increased DG in PFC, increased PA in AMY and increased GM1 in HIP in the DL group relative to HC group. The abundance of lipidomic subclasses in DL (red bars) were normalized by whose concentrations in HC group (blue bars). **(d-e)** Analysis of fatty acyl composition of DG species by total carbon chain length and total degree of unsaturation showed variation by brain region**.** The carbon chain length and unsaturation degree of DG ranged congruously in three brain regions, 34-40 and 2-5, respectively. The carbon chain length of DG altered in PFC, AMY and HIP; the unsaturation of DG altered in PFC n=6 per group. *P < 0.05, ** P < 0.01, ***P < 0.001, two-sided Student T-test; bars and points show mean ± SEM.

Fig.4 DG-related lipid pathway activity was particularly altered in the PFC of DL macaque. Analysis of lipid pathway activity showed altered predicted lipid fluxes occurred in brain regions. Calculated *Z*-scores were chosen to indicate the active/inactive pathways in DL relative to HC, with the positive/negative values.**(a)** The PFC of DL macaque showed major altered lipid pathways, which were 3 active pathways LPC-PC-PA-DG-TG, LPC-PC-PA-LPA and LPC-LPA, and 2 inactive pathway DG-PC-LPC, DG-PA-PI-LPI, respectively**.** Altered lipid pathway activity was calculated by *Z*-score of each lipid classes in DL(n=6) relative to HC(n=6). Red and blue arrows show reactions with positive and negative activity, respectively. Colored circles indicate the fold changes in lipid abundance between 2 groups (-0.47-1.0). Deep arrows indicate the shared lipid flux across the network. **(b-c)** The HIP of DL macaque showed minor altered lipid pathways, including active pathway LPC-LPA and inactive pathway LPA-PA-PG-LPG. **(d)** molecular geometric alteration of DG related lipid pathways. Blue and yellow backgrounds indicated head groups and hydrophobic part. Dashed frames showed the geometry of lipids molecule, which can be defined as cone (DG, PA, TG), cylinder (PC and PI) and inverted cone (LPI and LPC).

Fig.5 Network analyses of changed microbiome, DG in PFC and host phenotype interactions. The microbial species changed in DL were identified by LDA (LDA > 2), including14 bacterial and 33 viral species. Host-microbiota interaction network was built from Spearman's non-parametric rank correlation coefficient (P < 0.05), and showed with

coefficient >0.70 or <-0.70. Blue circles and V triangles indicate the altered bacteria and virus respectively, green rhombus indicate the DG species in PFC and red rhombus indicated the depressive behaviors. Edge-weighted Spring-Embedded Layout was used to cluster nodes in accordance with coefficient. In result, there were 3 clusters correlated with the behaviors that represent negative emotions and unhealthy effects (Huddle and Sit alone), mainly focused on bacterial family *Prevotellaceae* and viral families *Myoviridae* and *Siphoviridae.* There were 4 clusters correlated with behaviors that represent positive and healthy emotions (Locomotion and Communication), mainly focused on bacterial families *Gemella* and *Streptococcaceae* and viral families *Podoviridae* and *Siphoviridae.* No clusters correlated with Amicable behavior that represents positive and healthy emotions. Red and blue lines indicate the correlation coefficient and the color depth was consistent with the coefficient (-0.70 – 0.70).

Supplementary information

Addition file 1: Figure S1. Discriminating lipids in brain regions and plasma between HC and DL groups.

Addition file 2: Figure S2. Pathway activity of lipid showed changed reactions among brain regions in DL group relative to HC group.

Addition file 3: Table S1. Discriminatory gut virus between DL and HC groups.

Addition file 3: Table S2. Discriminatory bacterial species between DL and HC groups.

REFERENCES

1. Frankish H, Boyce N, Horton R. Mental health for all: a global goal. The Lancet. 2018;392**:**1493-1494.
2. Warden D, Rush AJ, Trivedi MH, Fava M, Wisniewski SR. The STAR*D Project results: a comprehensive review of findings. Curr Psychiatry Rep. 2007;9**:**449-459.
3. Ruelaz AR: *Treatment-resistant depression: Strategies for management.* 2006.
4. Sampson TR, Debelius JW, Thron T, Janssen S, Shastri GG, Ilhan ZE, et al. Gut Microbiota Regulate Motor Deficits and Neuroinflammation in a Model of Parkinson's Disease. Cell. 2016;167**:**1469-1480 e1412.
5. Hsiao EY, McBride SW, Hsien S, Sharon G, Hyde ER, McCue T, et al. The microbiota modulates gut physiology and behavioral abnormalities associated with autism. Cell. 2013;155**:**1451.
6. Hu S, Li A, Huang T, Lai J, Li J, Sublette ME, et al. Gut Microbiota Changes in Patients with Bipolar Depression. Adv Sci (Weinh). 2019;6**:**1900752.
7. Zheng P, Zeng B, Liu M, Chen J, Pan J, Han Y, et al. The gut microbiome from patients with schizophrenia modulates the glutamate-glutamine-GABA cycle and schizophrenia-relevant behaviors in mice. Science advances. 2019;5**:**eaau8317.
8. Zheng P, Wu J, Zhang H, Perry SW, Yin B, Tan X, et al. The gut microbiome modulates gut-brain axis glycerophospholipid metabolism in a region-specific manner in a nonhuman primate model of depression. Mol Psychiatry. 2020;
9. Sapolsky RM. The influence of social hierarchy on primate health. Science. 2005;308**:**648-652.
10. Chen JJ, Xie J, Zeng BH, Li WW, Bai SJ, Zhou C, et al. Absence of gut microbiota affects lipid

metabolism in the prefrontal cortex of mice. Neurol Res. 2019;41:1104-1112.
11. Nicholson JK, Holmes E, Kinross J, Burcelin R, Gibson G, Jia W, et al. Host-gut microbiota metabolic interactions. Science. 2012;336:1262-1267.
12. Zhu L, Zhong M, Elder GA, Sano M, Holtzman DM, Gandy S, et al. Phospholipid dysregulation contributes to ApoE4-associated cognitive deficits in Alzheimer's disease pathogenesis. Proc Natl Acad Sci U S A. 2015;112:11965-11970.
13. Kurian MA, Meyer E, Vassallo G, Morgan NV, Prakash N, Pasha S, et al. Phospholipase C beta 1 deficiency is associated with early-onset epileptic encephalopathy. Brain. 2010;133:2964-2970.
14. Lauwers E, Goodchild R, Verstreken P. Membrane Lipids in Presynaptic Function and Disease. Neuron. 2016;90:11-25.
15. Davletov B, Montecucco C. Lipid function at synapses. Curr Opin Neurobiol. 2010;20:543-549.
16. Puchkov D, Haucke V. Greasing the synaptic vesicle cycle by membrane lipids. Trends Cell Biol. 2013;23:493-503.
17. Kikuchi T, Morizane A, Doi D, Magotani H, Onoe H, Hayashi T, et al. Human iPS cell-derived dopaminergic neurons function in a primate Parkinson's disease model. Nature. 2017;548:592-596.
18. Chu X. Preliminary validation of natural depression in macaques with acute treatments of the fast-acting antidepressant ketamine. Behav Brain Res. 2019;360:60-68.
19. Li X, Xu F, Xie L, Ji Y, Cheng K, Zhou Q, et al. Depression-Like Behavioral Phenotypes by Social and Social Plus Visual Isolation in the Adult Female Macaca fascicularis. PLoS ONE. 2013;8:: e73293.
20. Xu F, Wu Q, Xie L, Gong W, Zhang J, Zheng P, et al. Macaques exhibit a naturally-occurring depression similar to humans. Sci Rep. 2015;5:9220.
21. Dijkman K, Sombroek CC, Vervenne RAW, Hofman SO, Boot C, Remarque EJ, et al. Prevention of tuberculosis infection and disease by local BCG in repeatedly exposed rhesus macaques. Nat Med. 2019;25:255-262.
22. Sorrells SF, Paredes MF, Cebrian-Silla A, Sandoval K, Qi D, Kelley KW, et al. Human hippocampal neurogenesis drops sharply in children to undetectable levels in adults. Nature. 2018;555:377-381.
23. Saleem KS, Logothetis NK: *A combined MRI and histology atlas of the rhesus monkey brain in stereotaxic coordinates.* Academic Press; 2012.
24. NeuroMaps. [http://braininfo.rprc.washington.edu/], 2016, Accessed on Date 2016
25. Zheng P, Zeng B, Zhou C, Liu M, Fang Z, Xu X, et al. Gut microbiome remodeling induces depressive-like behaviors through a pathway mediated by the host's metabolism. Mol Psychiatry. 2016;21:786-796.
26. Zheng P, Zeng B, Liu M, Chen J, Pan J, Han Y, et al. The gut microbiome from patients with schizophrenia modulates the glutamate-glutamine-GABA cycle and schizophrenia-relevant behaviors in mice. Sci Adv. 2019;5:eaau8317.
27. Ugurel S, Schrama D, Keller G, Schadendorf D, Brocker EB, Houben R, et al. Impact of the CCR5 gene polymorphism on the survival of metastatic melanoma patients receiving immunotherapy. Cancer Immunol Immunother. 2008;57:685-691.
28. Li D, Liu C-M, Luo R, Sadakane K, Lam T-W. MEGAHIT: an ultra-fast single-node solution for large

and complex metagenomics assembly via succinct de Bruijn graph. Bioinformatics. 2015;31:1674-1676.
29. Fu L, Niu B, Zhu Z, Wu S, Li W. CD-HIT: accelerated for clustering the next-generation sequencing data. Bioinformatics. 2012;28:3150-3152.
30. Li R, Li Y, Kristiansen K, Wang J. SOAP: short oligonucleotide alignment program. Bioinformatics. 2008;24:713-714.
31. Altschul SF, Madden TL, Schäffer AA, Zhang J, Zhang Z, Miller W, et al. Gapped BLAST and PSI-BLAST: a new generation of protein database search programs. Nucleic acids research. 1997;25:3389-3402.
32. Zhang D, Jing X, Yang J: *Biometric image discrimination technologies.* IGI Global; 2006.
33. Bradley W, Steven H, Robert P. Utilities for quantifying separation in PCA/PLS-DA scores plots. Anal Biochem. 2013;433:102-104.
34. Nguyen A, Rudge SA, Zhang Q, Wakelam MJ. Using lipidomics analysis to determine signalling and metabolic changes in cells. Curr Opin Biotechnol. 2017;43:96-103.
35. Hahn O, Drews LF, Nguyen A, Tatsuta T, Gkioni L, Hendrich O, et al. A nutritional memory effect counteracts benefits of dietary restriction in old mice. Nat Metab. 2019;1:1059-1073.
36. Yang J, Zheng P, Li Y, Wu J, Tan X, Zhou J, et al. Landscapes of bacterial and metabolic signatures and their interaction in major depressive disorders. Science Advances. 2020;6 : eaba8555:
37. Barandouzi ZA, Starkweather AR, Henderson WA, Gyamfi A, Cong XS. Altered Composition of Gut Microbiota in Depression: A Systematic Review. Front Psychiatry. 2020;11:541.
38. Liskiewicz P, Kaczmarczyk M, Misiak B, Wronski M, Baba-Kubis A, Skonieczna-Zydecka K, et al. Analysis of gut microbiota and intestinal integrity markers of inpatients with major depressive disorder. Prog Neuropsychopharmacol Biol Psychiatry. 2020;110076.
39. Wan L, Ge WR, Zhang S, Sun YL, Wang B, Yang G. Case-Control Study of the Effects of Gut Microbiota Composition on Neurotransmitter Metabolic Pathways in Children With Attention Deficit Hyperactivity Disorder. Front Neurosci. 2020;14:127.
40. Lu CC, Hu ZB, Wang R, Hong ZH, Lu J, Chen PP, et al. Gut microbiota dysbiosis-induced activation of the intrarenal renin-angiotensin system is involved in kidney injuries in rat diabetic nephropathy. Acta Pharmacol Sin. 2020;41:1111-1118.
41. Colica C, Avolio E, Bollero P, Costa de Miranda R, Ferraro S, Sinibaldi Salimei P, et al. Evidences of a New Psychobiotic Formulation on Body Composition and Anxiety. Mediators Inflamm. 2017;2017:5650627.
42. Simren M, Ohman L, Olsson J, Svensson U, Ohlson K, Posserud I, et al. Clinical trial: the effects of a fermented milk containing three probiotic bacteria in patients with irritable bowel syndrome - a randomized, double-blind, controlled study. Aliment Pharmacol Ther. 2010;31:218-227.
43. Marcos A, Warnberg J, Nova E, Gomez S, Alvarez A, Alvarez R, et al. The effect of milk fermented by yogurt cultures plus Lactobacillus casei DN-114001 on the immune response of subjects under academic examination stress. Eur J Nutr. 2004;43:381-389.
44. Bozek K, Wei Y, Yan Z, Liu X, Xiong J, Sugimoto M, et al. Organization and evolution of brain lipidome revealed by large-scale analysis of human, chimpanzee, macaque, and mouse tissues. Neuron. 2015;85:695-702.

45. Yadav RS, Tiwari NK. Lipid integration in neurodegeneration: an overview of Alzheimer's disease. Mol Neurobiol. 2014;50:168-176.
46. Kornhuber J, Rhein C, Müller CP, Mühle C. Secretory sphingomyelinase in health and disease. Biol Chem. 2015;396:707-736.
47. Adibhatla RM, Hatcher JF. Phospholipase A(2), reactive oxygen species, and lipid peroxidation in CNS pathologies. BMB Rep. 2008;41:560-567.
48. Liu X, Li J, Zheng P, Zhao X, Zhou C, Hu C, et al. Plasma lipidomics reveals potential lipid markers of major depressive disorder. Anal Bioanal Chem. 2016;408:6497-6507.
49. Liu X, Zheng P, Zhao X, Zhang Y, Hu C, Li J, et al. Discovery and validation of plasma biomarkers for major depressive disorder classification based on liquid chromatography-mass spectrometry. J Proteome Res. 2015;14:2322-2330.
50. Zheng P, Gao HC, Li Q, Shao WH, Zhang ML, Cheng K, et al. Plasma metabonomics as a novel diagnostic approach for major depressive disorder. J Proteome Res. 2012;11:1741-1748.
51. Jia HM, Li Q, Zhou C, Yu M, Yang Y, Zhang HW, et al. Chronic unpredictive mild stress leads to altered hepatic metabolic profile and gene expression. Sci Rep. 2016;6:23441.
52. Kulig W, Korolainen H, Zatorska M, Kwolek U, Wydro P, Kepczynski M, et al. Complex Behavior of Phosphatidylcholine-Phosphatidic Acid Bilayers and Monolayers: Effect of Acyl Chain Unsaturation. Langmuir. 2019;35:5944-5956.
53. Postila PA, Rog T. A Perspective: Active Role of Lipids in Neurotransmitter Dynamics. Mol Neurobiol. 2020;57:910-925.
54. Oliveira TG, Chan RB, Bravo FV, Miranda A, Silva RR, Zhou B, et al. The impact of chronic stress on the rat brain lipidome. Mol Psychiatry. 2016;21:80-88.
55. Sliz E, Shin J, Syme C, Black S, Seshadri S, Paus T, et al. Thickness of the cerebral cortex shows positive association with blood levels of triacylglycerols carrying 18-carbon fatty acids. Commun Biol. 2020;3:456.
56. Levental KR, Malmberg E, Symons JL, Fan YY, Chapkin RS, Ernst R, et al. Lipidomic and biophysical homeostasis of mammalian membranes counteracts dietary lipid perturbations to maintain cellular fitness. Nat Commun. 2020;11:1339.
57. Loeffler JM, Nelson D, Fischetti VA. Rapid killing of Streptococcus pneumoniae with a bacteriophage cell wall hydrolase. Science. 2001;294:2170-2172.
58. Romero P, Lopez R, Garcia E. Characterization of LytA-like N-acetylmuramoyl-L-alanine amidases from two new Streptococcus mitis bacteriophages provides insights into the properties of the major pneumococcal autolysin. J Bacteriol. 2004;186:8229-8239.
59. van der Burg KP, Cribb L, Firth J, Karmacoska D, Mischoulon D, Byrne GJ, et al. EPA and DHA as markers of nutraceutical treatment response in major depressive disorder. Eur J Nutr. 2020;59:2439-2447.
60. Weiser MJ, Wynalda K, Salem N, Jr., Butt CM. Dietary DHA during development affects depression-like behaviors and biomarkers that emerge after puberty in adolescent rats. J Lipid Res. 2015;56:151-166.
61. Weatheall D. The use of non-human primates in research. London: Academy of Medical Sciences. 2006;

Figures

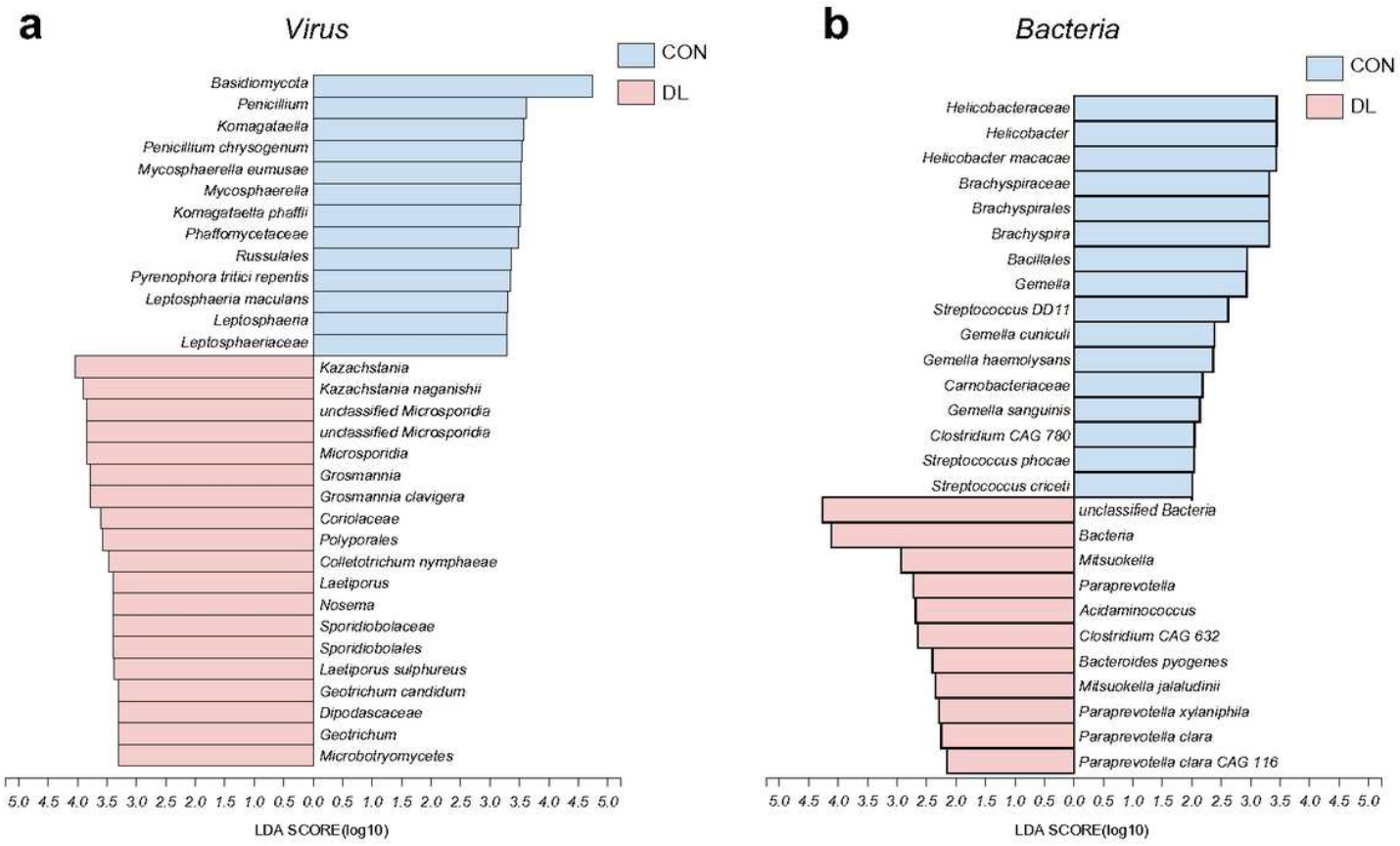

Figure 1

The virus and bacteria that discriminate DL from HC groups LEfSe of bacteria and virus from phylum to species level. Linear discriminant analysis (LDA) combined with effect size measurements revealed a list of features that enable discrimination between the HC and DL groups in the fecal samples. a. At the viral level, the DL subjects showed 16 enriched species, mainly belonging to families Myoviridae (7 species) and Siphoviridae (4 species), and 17 depleted species mainly from the families Podoviridae (6 species) and Siphoviridae (6 species). b. At the bacterial level, the DL subjects showed 6 enriched species, mainly belonging to family Paraprevotella (3 species), and 8 depleted species mainly from the families Streptococcaceae (3 species) and Gemella (3 species). The discriminative variants (gut virus, bacteria species) were identified based on LDA score > 2.5. Sample set: HC, n = 6; DL, n = 6.

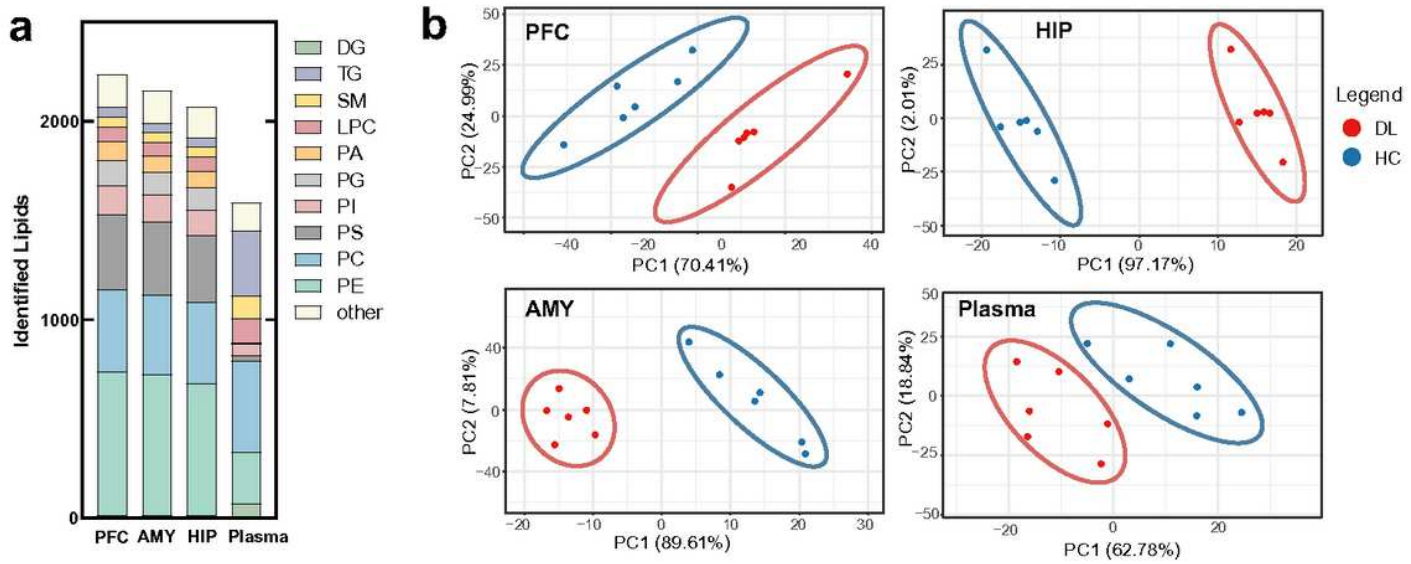

Figure 2

Profile of lipidomic changes in brain and plasma. a. Composition of subclasses of total identified lipids in prefrontal cortex (PFC), amygdala (AMY), hippocampus (HIP) and plasma. Identified lipids exhibited similar composition of subclasses in 3 brain regions (2238, 2153, 2074, respectively). b. Partial Least Squares Discriminant Analysis (PLS-DA) showed that the PFC, HIP, AMY and plasma metabolic signatures of DL group were substantially different from that in the HC group (n=6, HC, blue dots; n=6, DL, red dots). PC, Phosphatidylcholine; PE, Phosphatidylethanolamine; Cer, ceramide; LPE, lyso-Phosphatidylethanolamine; PA, phosphatidic acids; PG, phosphatidylglycerols; PI, phosphatidylinositols; PS, phosphatidylserines; SM, sphingmyelin; DG, 1,2-Diacylglycerol; LPC, 2-Lysophosphatidylcholine; So, sphingosine; TG, Triacylglycerol.

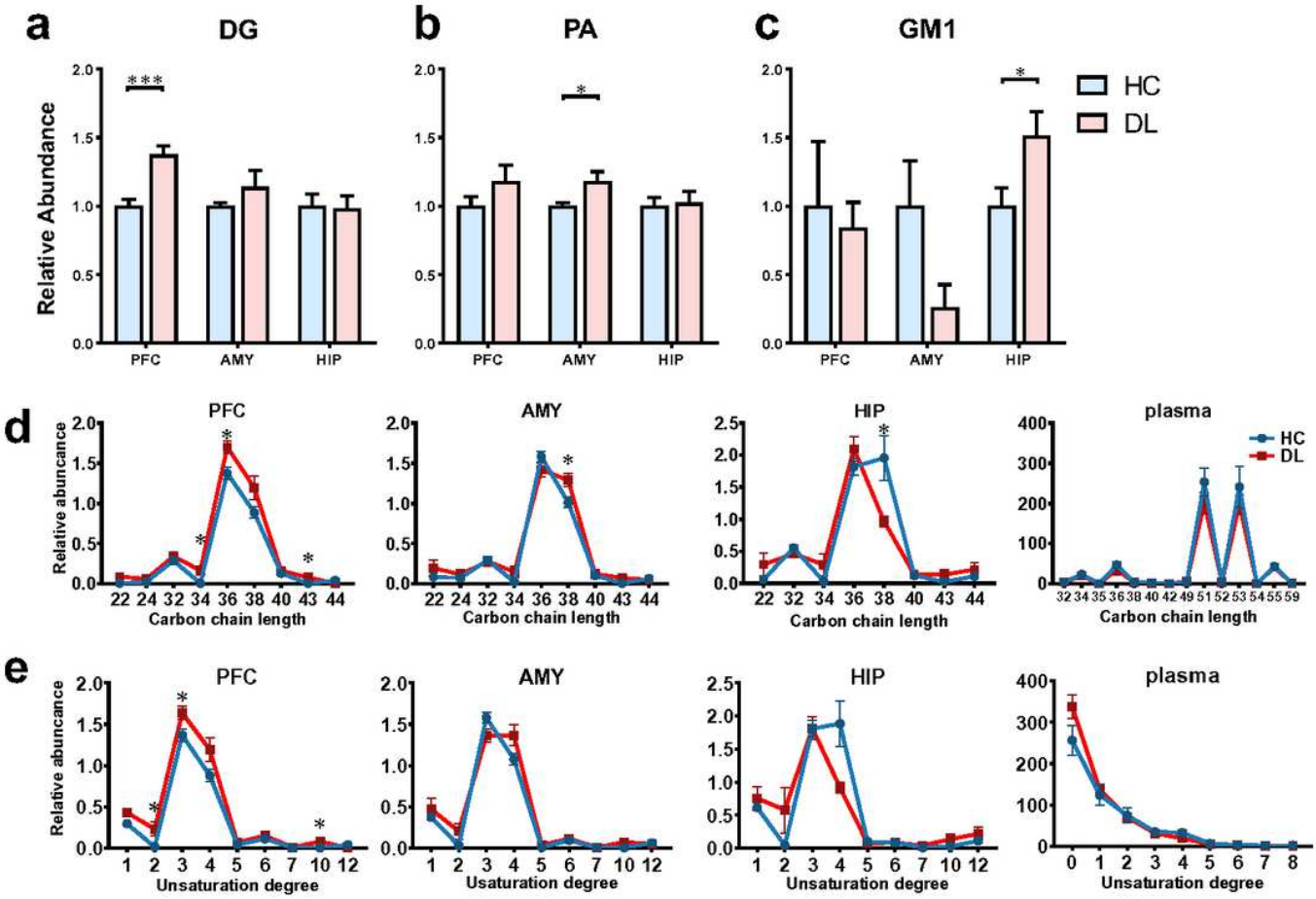

Figure 3

Significant changes exhibited in abundance and fatty acid composition of 1,2-Diacylglycerol (DG) in the PFC of DL macaques. (a-c) The abundance of some lipidomic subclasses showed significantly changes with specific brain regions, displaying the increased DG in PFC, increased PA in AMY and increased GM1 in HIP in the DL group relative to HC group. The abundance of lipidomic subclasses in DL (red bars) were normalized by whose concentrations in HC group (blue bars). (d-e) Analysis of fatty acyl composition of DG species by total carbon chain length and total degree of unsaturation showed variation by brain region. The carbon chain length and unsaturation degree of DG ranged congruously in three brain regions, 34-40 and 2-5, respectively. The carbon chain length of DG altered in PFC, AMY and HIP; the unsaturation of DG altered in PFC n=6 per group. *P < 0.05, ** P < 0.01, ***P < 0.001, two-sided Student T-test; bars and points show mean ± SEM.

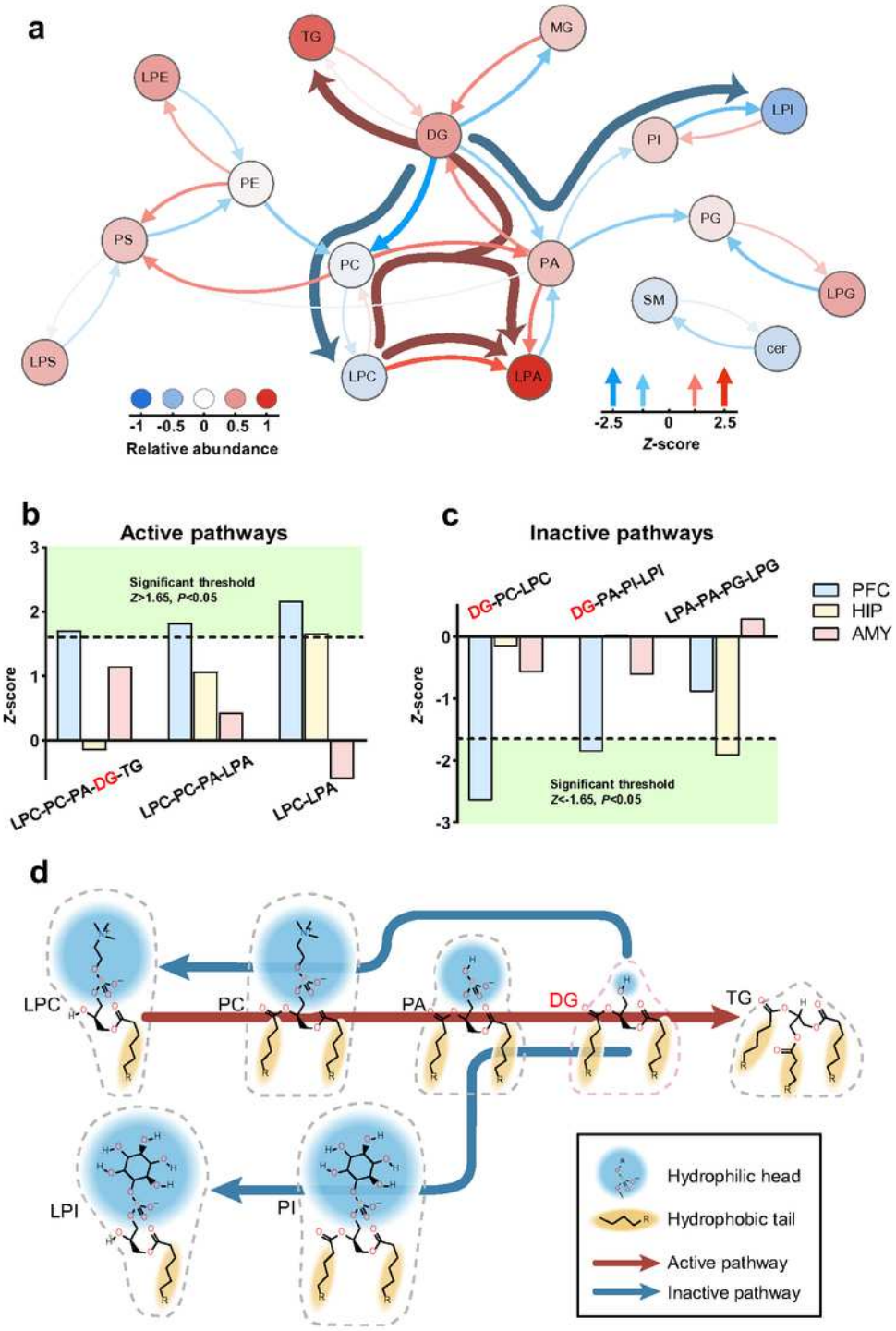

Figure 4

DG-related lipid pathway activity was particularly altered in the PFC of DL macaque. Analysis of lipid pathway activity showed altered predicted lipid fluxes occurred in brain regions. Calculated Z-scores were chosen to indicate the active/inactive pathways in DL relative to HC, with the positive/negative values.(a) The PFC of DL macaque showed major altered lipid pathways, which were 3 active pathways LPC-PC-PA-DG-TG, LPC-PC-PA-LPA and LPC-LPA, and 2 inactive pathway DG-PC-LPC, DG-PA-PI-LPI, respectively.

Altered lipid pathway activity was calculated by Z-score of each lipid classes in DL(n=6) relative to HC(n=6). Red and blue arrows show reactions with positive and negative activity, respectively. Colored circles indicate the fold changes in lipid abundance between 2 groups (-0.47-1.0). Deep arrows indicate the shared lipid flux across the network. (b-c) The HIP of DL macaque showed minor altered lipid pathways, including active pathway LPC-LPA and inactive pathway LPA-PA-PG-LPG. (d) molecular geometric alteration of DG related lipid pathways. Blue and yellow backgrounds indicated head groups and hydrophobic part. Dashed frames showed the geometry of lipids molecule, which can be defined as cone (DG, PA, TG), cylinder (PC and PI) and inverted cone (LPI and LPC).

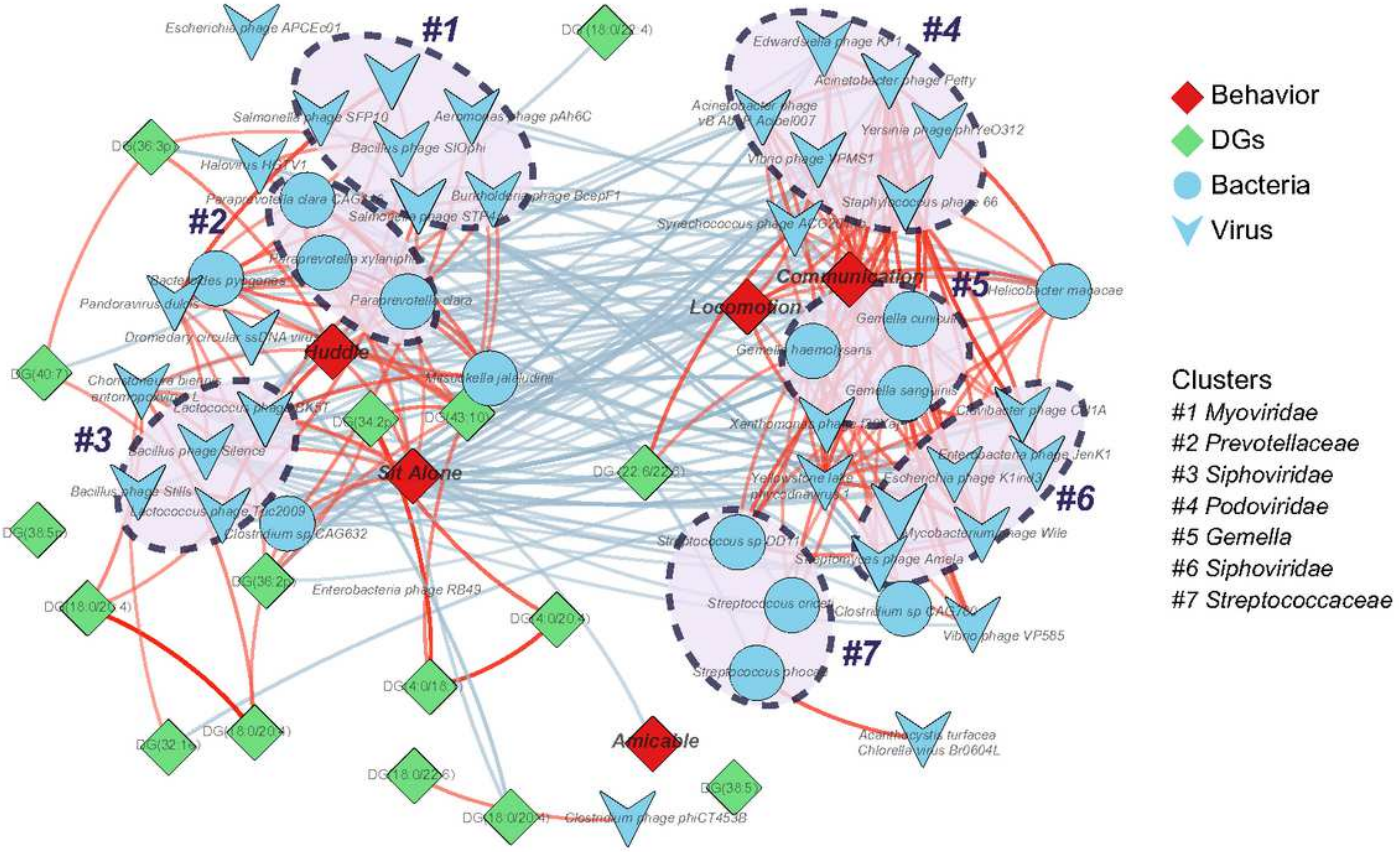

Figure 5

Network analyses of changed microbiome, DG in PFC and host phenotype interactions. The microbial species changed in DL were identified by LDA (LDA > 2), including14 bacterial and 33 viral species. Host-microbiota interaction network was built from Spearman's non-parametric rank correlation coefficient ($P < 0.05$), and showed with coefficient >0.70 or <-0.70. Blue circles and V triangles indicate the altered bacteria and virus respectively, green rhombus indicate the DG species in PFC and red rhombus indicated the depressive behaviors. Edge-weighted Spring-Embedded Layout was used to cluster nodes in

accordance with coefficient. In result, there were 3 clusters correlated with the behaviors that represent negative emotions and unhealthy effects (Huddle and Sit alone), mainly focused on bacterial family Prevotellaceae and viral families Myoviridae and Siphoviridae. There were 4 clusters correlated with behaviors that represent positive and healthy emotions (Locomotion and Communication), mainly focused on bacterial families Gemella and Streptococcaceae and viral families Podoviridae and Siphoviridae. No clusters correlated with Amicable behavior that represents positive and healthy emotions. Red and blue lines indicate the correlation coefficient and the color depth was consistent with the coefficient (-0.70 – 0.70).

Supplementary Files

This is a list of supplementary files associated with this preprint. Click to download.

- Additionfile1.docx
- Additionfile2.docx
- Additionfile3.docx
- Additionfile4.docx
- workflow.pdf